Angewandte Chemie
Eine Zeitschrift der Gesellschaft Deutscher Chemiker

Supporting Information

69451 Weinheim, Germany

Direct Arithmetic by the Position of the Wheel on the Axle: Half-Adder Based on a Photo-Driven [2]Rotaxane

Da-Hui Qu, Qiao-Chun Wang, and He Tian*

Lab for Advanced Materials and Institute of Fine Chemicals, East China University of Science & Technology, Shanghai 200237, P.R. China, Fax: (+86)-21-64252288

E-mail: tianhe@ecust.edu.cn

General: H NMR spectra were measured on a Brücker AM 500 spectrometer. Elemental analysis was performed on a Perkin-Elmer 2400C instrument. MALDI-TOF spectrum was recorded a 4700-Propeomics analyzer. UV/Vis spectra were done on a Varian Cary 500 spectrophotometer (1-cm quartz cell used) at 25 ºC. Fluorescent spectra were recorded on a Varian Cary Eclipse Fluorescence Spectrophotometer (1-cm quartz cell used) at 25 ºC. The photo-irradiation was carried on a CHF-XM 500-W high-pressure mercury lamp with suitable filters (313 nm, 280 nm, 380 nm, type FAL, made in Germany) in a sealed Ar-saturated 1 cm quartz cell. The distance between the lamp and the sample cell is 20 cm.

Experimental Section

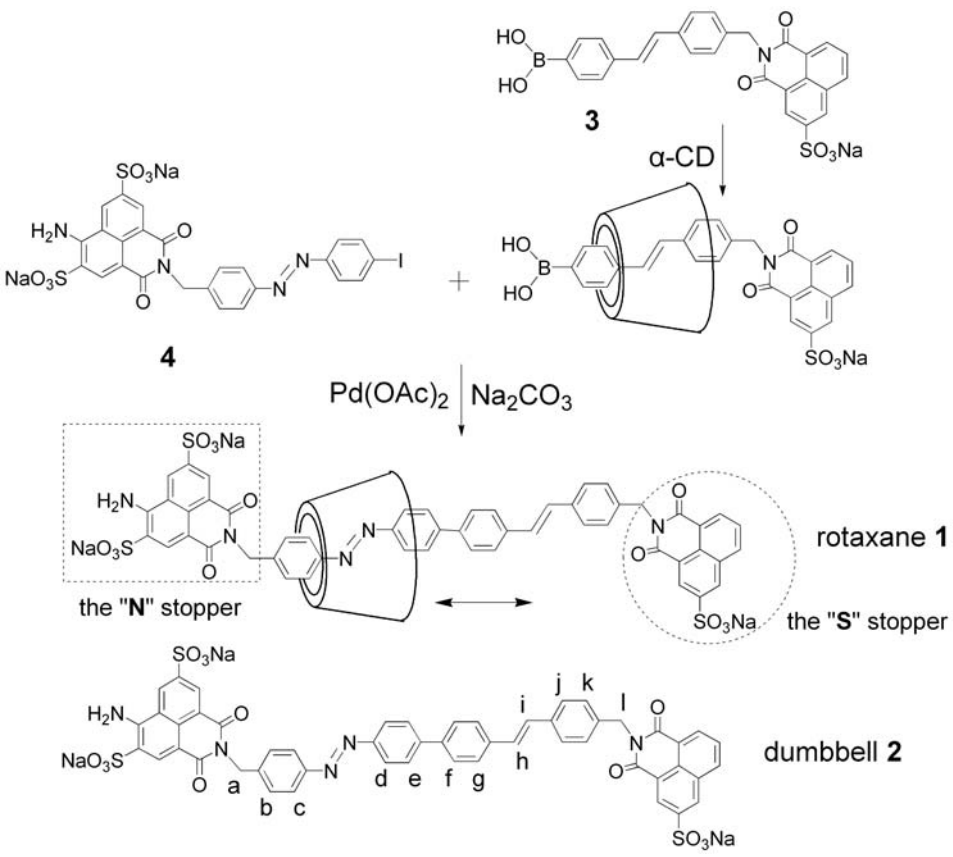

Figure S1. The synthetic routine of [2]rotaxane **1**.

[2]rotaxane **1:** Compound **3**, compound **4** and dumbbell **2** were prepared as described previously.[S1] Compound **3** (0.054 g, 0.10 mmol), α-CD (0.11 g, 0.13 mmol), dissolved in DMSO (5 mL) and Ar-saturated sodium carbonate aqueous solution (20 mL, 0.2 mol/L), then the mixture was stirred at 85 ºC for 20 h. Palladium(Ⅱ) acetate (4.0 mg, 0.019 mmol) and compound **4** (0.083 g, 0.11 mmol) were added and stirred at 85 ºC for 24 h, then cooled and acidified with acetic acid, after concentrated in vacuo, the resulting dark solid was purified by column chromatography (silica gel, the upper layer of 1.3:2:5 acetic acid/n-butanol/water) to give pure **1** (45 mg, 21.5%) as yellow powder. M.p.> 250ºC; ^{1}H NMR (500 MHz, [D_6]-DMSO, 25 ºC, TMS): δ= 8.98 (s, 1H), 8.72 (s, 1H), 8.70 (s, 1H), 8.69 (s, 1H), 8.65 (s, 1H), 8.58 (d, J=8.2 Hz,

1H), 8.54 (d, J=7.2 Hz, 1H), 8.02 (s, 2H), 8.0 (d, J=8.0 Hz, 2H), 7.97 (d, J=8.1 Hz, 2H), 7.90 (m, 5H), 7.85 (d, J=7.7 Hz, 2H), 7.75 (d, J=7.7 Hz, 2H), 7.52 (d, J=8.1 Hz, 2H), 7.41 (d, J=8.1 Hz 2H), 7.14 (d, J=16.1 Hz, 1H), 7.01 (d, J=16.1 Hz, 1H), 5.38 (s, 12H), 5.28 (s, 4H), 4.70 (s, 6H), 4.40 (s, 6H), 3.64 (m, 6H), 3.48 (m, 18H), 3.3 (m, 6H), 3.18 (m, 6H); MALDI-TOF: m/z (%): 2095.4 (100) [M^++Na], 2072.4 (58) [M^+]; elemental analysis calcd (%) for $C_{88}H_{92}N_5Na_3O_{43}S_3 \cdot 6H_2O$: C 48.46, H 4.81, N 3.21; found C 48.48, H 4.80, N 3.22.

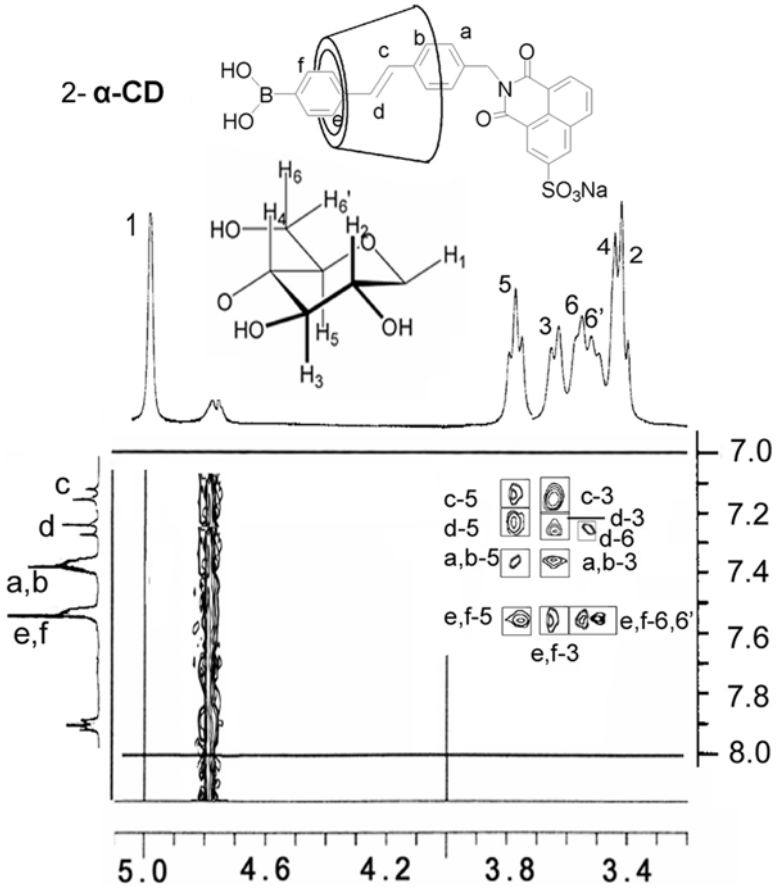

Figure S2. The two-dimensional ROESY NMR spectrum of **2-α-CD** (500 MHz in D_2O at 298 K) at a mixing time of 300 ms. The NOEs between the aromatic protons and H3, H5 and H6 protons on the interior of the α-CD annulus were found (from H_a, H_b, H_c, H_d to H3 and from H_c, H_d, H_e, H_f to H5 and from H_e, H_f to H6). The dominant configuration is also that the wide 2,3-rim is near to the stopper.

The ^{1}H NMR and two-dimensional ROESY NMR spectra of *E, Z1, Z2, Z3*-1

Irradiation at 380 nm leads to two new signals of equal intensity for H_c and H_d (Figure S3b) appearing at δ=6.67 and 6.82 ppm, respectively, correspondingly the initial peaks appearing at δ=7.90 and 7.97 ppm. Also, change in the resonance of the methylene protons (δ=5.28, $H_{a,l}$) was profound. Before the irradiation by 380 nm, the chemical shifts of the proton H_a and H_l are equal. The irradiation with 380 nm causes the splitting of the proton peak into one doublet and one singlet as compared to one singlet peak before the irradiation. A new signal was found at δ=5.41 (H_l of *Z1*-**1**). The ratio of the integrals of the two signals of H_d suggest that at the photostationary state of azobenzene isomerization (namely **PSS-Z1**) about 65% of *E*-**1** was transformed to *Z1*-**1** isomer.

Irradiation by 313 nm on *E*-**1** results in the fact that the signals of aromatic protons of stilbene unit generally shift to upfields, for H_h, H_i (Figure S3c) appearing at δ=6.5~6.7 (initially δ=7.0~7.2), H_j appearing at δ 6.55 (initially δ=7.41), H_g appearing at δ=7.12 (initially δ=7.52). The resonance of the methylene protons are also split, in which the signal of H_a represents a doublet at δ=5.42. Also, the coupling constant in the *cis*-stilbene protons H_h and H_i in Figure S3c (14.5 Hz) is smaller than that in the *trans*-stilbene protons H_h and H_i in Figure S3a (16.1 Hz). The ratio of the integrals of the two signals of H_h suggest that at the photostationary state of the stilbene isomerization (namely **PSS-Z2**) about 60% of *E*-**1** was transformed to *Z2*-**1** isomer in that case. Irradiation by 313 nm on *Z1*-**1** or irradiation by 380 nm on *Z2*-**1** results in the fact that the signals of aromatic protons of stilbene unit and azobenzene unit

generally shift to upfields similarly (Figure S3d), indicating generation of *Z3*-**1**. At the photostationary state of the stilbene and azobenzene isomerizations (namely **PSS-Z3**) there is about 34% of *Z3*-**1** in the system.

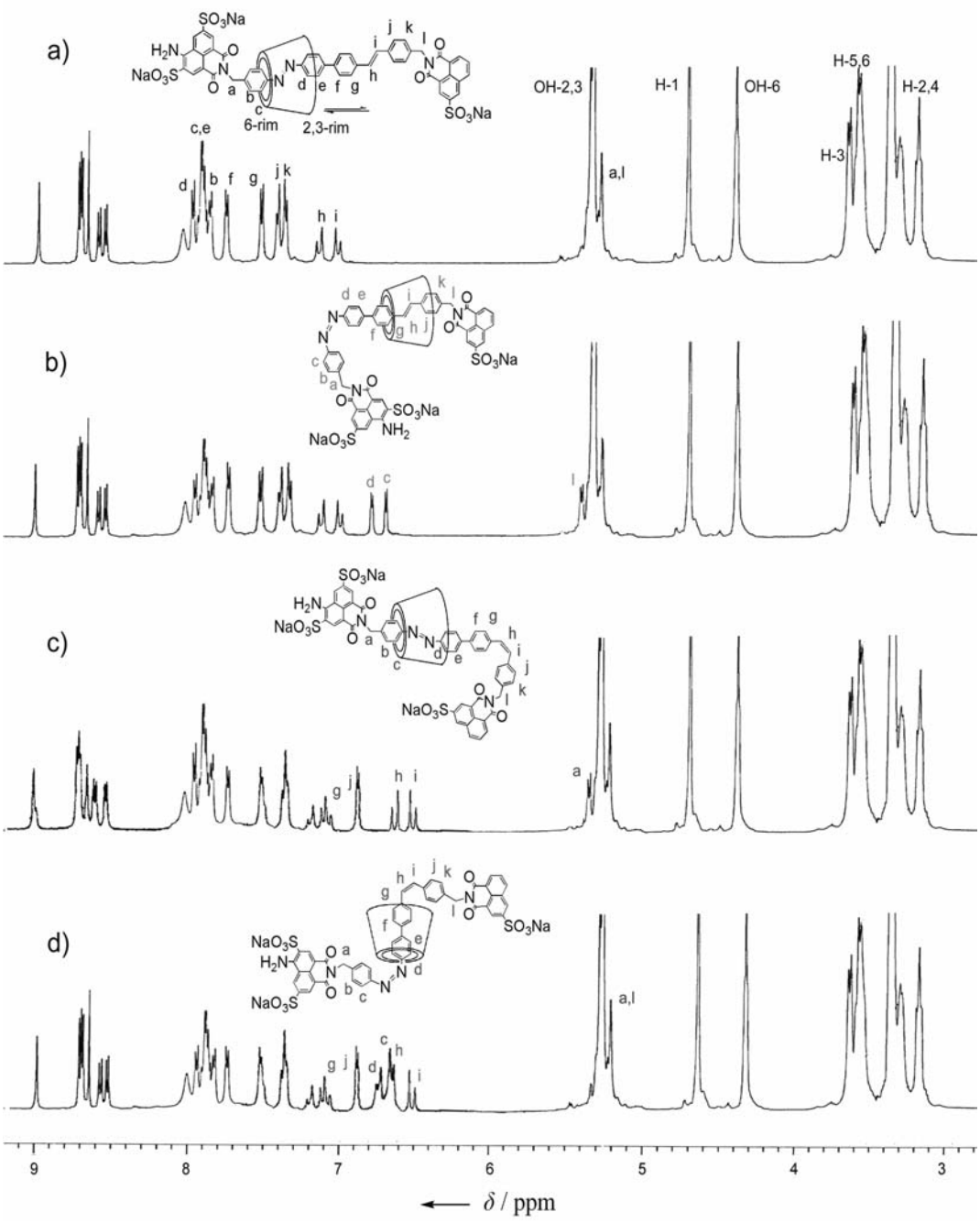

Figure S3. ^{1}H NMR spectra (500 MHz in [D_6]DMSO at 298 K) of (a) [2]rotaxane **1**; (b) *Z1*-**1**, irradiation on *E*-**1** by 380 nm for 2 h; (c) *Z2*-**1**, irradiation on *E*-**1** by 313 nm for 3 h; (d) *Z3*-**1**, irradiation on *E*-**1** by 380 nm for 2 h, then irradiation at 313 nm for 3 h.

Rotaxane *E*-**1** is at a dynamic state at room temperature in d_6-DMSO in that the α-CD bead moves back and forward between the azobenzene station and the stilbene station. In *E* isomer, NOEs (Figure S4) are observed from protons H_b-H_k on the dumbbell to the internal protons H3, H5, and H6 of α-CD. This set of NOEs is not consistent with any single static geometry, and shows that the cyclodextrin rapidly glides up and down the dumbbell. NOEs are observed from H_b, H_c to OH-6 of the cyclodextrin (but no NOEs from H_b, H_c to OH-2, 3) and from H_j, H_k to OH-2,3 of the cyclodextrin (but no from H_b, H_c to OH-6), which also proves that the orientation of α-CD is coincident with that shown in Figure 1 (**DS-E**). Irradiation by 380 nm on *E*-**1** caused the photoisomerization of the azobenzene unit, which generates *Z1*-**1**. A completely different pattern of NOEs (Figure S5) is observed in the *Z1* isomer. Here the NOEs are more selective, and the NOEs from the protons of the stilbene unit to the protons of α-CD are much stronger than these from the protons of the azobenzene unit. All these NOEs are consistent with the geometry of the *Z1* isomer shown in Figure 1, where the α-CD ring stays at the stilbene unit (**PSS-Z1**). Irradiation by 313 nm on *E*-**1** caused the photoisomerization of the stilbene unit, which generates *Z2*-**1**. The NOEs are more selective, and the NOEs from the protons of the azobenzene unit to the protons of α-CD are much stronger than these from the protons of the stilbene unit (Figure S6). All these NOEs are consistent with the geometry of the *Z2* isomer shown in Figure 1, where the α-CD ring stays at the azobenzene unit (**PSS-Z2**). Irradiation by 313 nm on *Z1*-**1** can generate *Z3*-**1**. A completely different pattern of NOEs is observed in the *Z3* isomer relatively to the *E* isomer. Here the NOEs are also

more selective. Strong NOEs are observed from the protons of the biphenyl unit and the protons H3, H5 of α-CD (Figure S7), which can indicate that the structure of rotaxane **1** are consistent with the geometry of the *Z3* isomer, where the α-CD ring stays at the biphenyl unit (**PSS-Z3**).

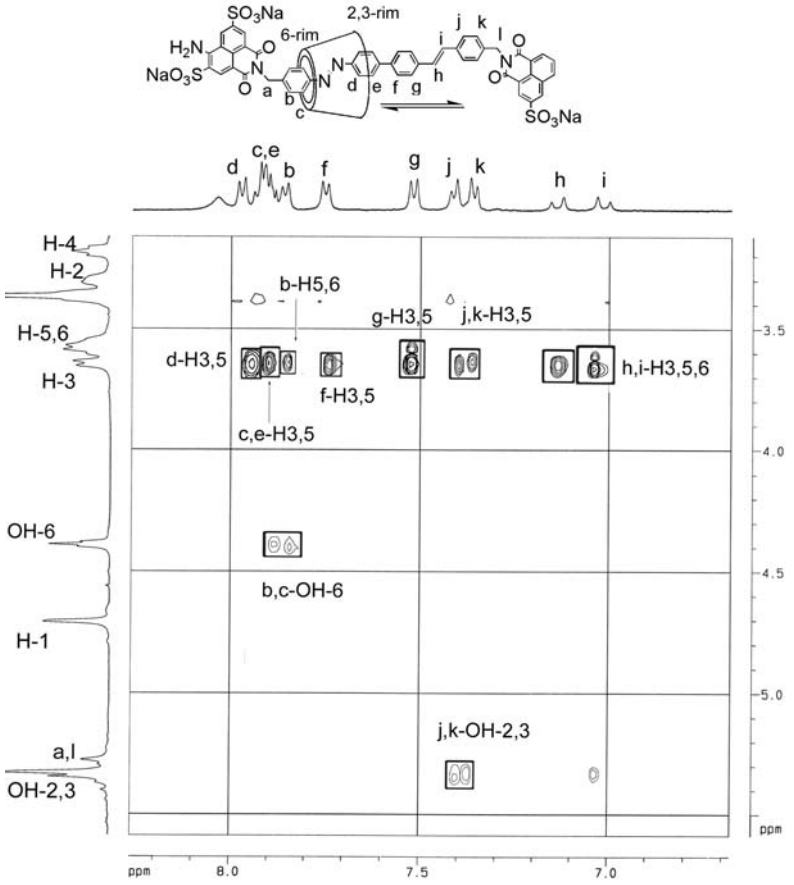

Figure S4. The two-dimensional ^{1}H ROESY NMR spectrum of *E*-**1** (500 MHz in [D_6]-DMSO at 298 K, at a mixing time of 300 ms).

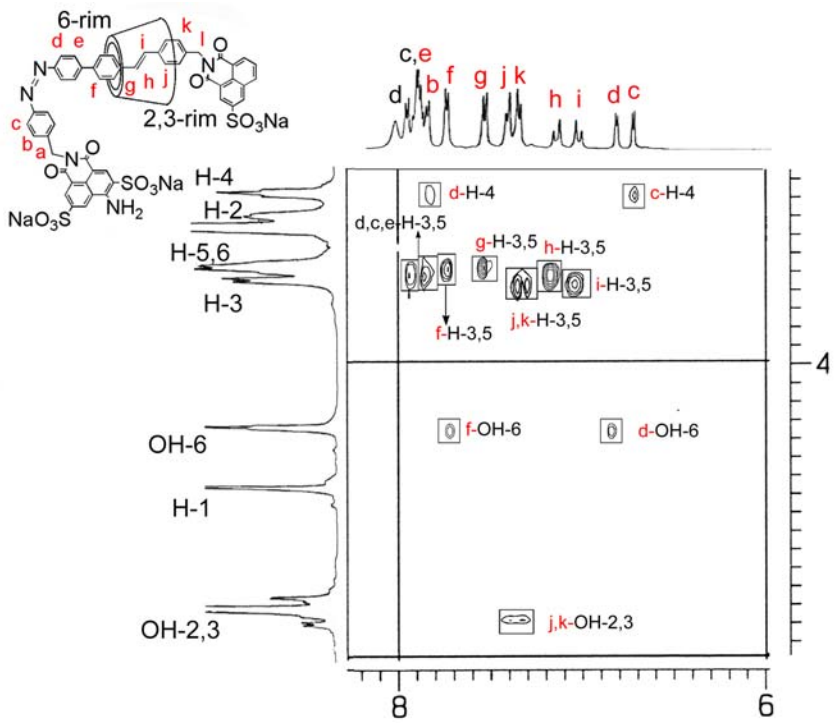

Figure S5 The two-dimensional ^{1}H ROESY NMR spectrum (500 MHz in [D_6]-DMSO at 298 K, at a mixing time of 300 ms) of *Z1*-**1** (*E*-**1** after irradiation at 380 nm for 2 h).

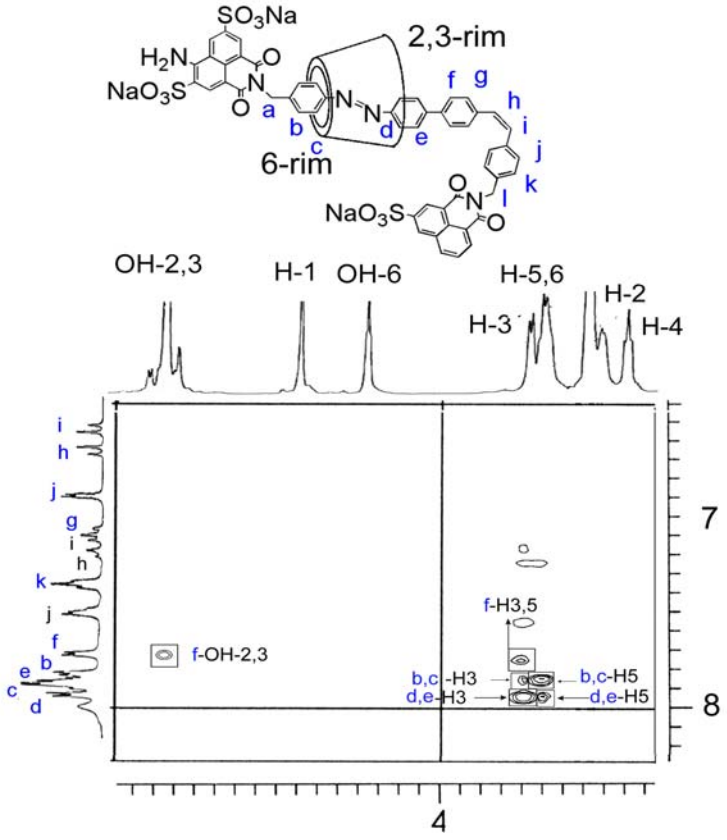

Figure S6. The two-dimensional ^{1}H ROESY NMR spectrum (500 MHz in [D_6]-DMSO at 298 K, at a mixing time of 300 ms) of *Z2*-**1** (*E*-**1** after irradiation at 313 nm for 3 h).

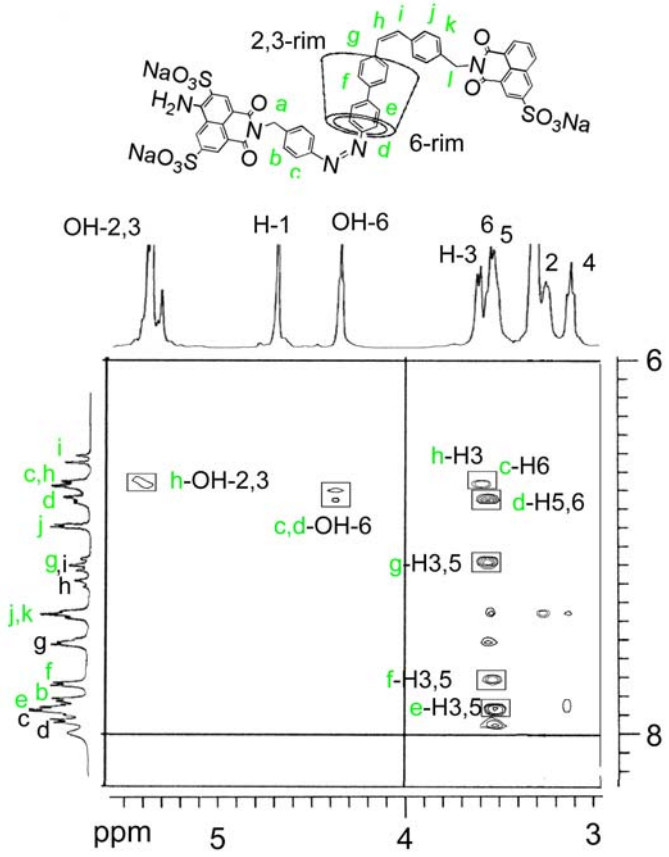

Figure S7. The two-dimensional ^{1}H ROESY NMR spectrum (500 MHz in [D_6]-DMSO at 298 K, at a mixing time of 300 ms) of *Z3*-**1**. (*E*-**1** after irradiation at 313 nm for 3 h, then irradiated at 380 nm for 2 h).

Absorption spectra of dumbbell 2 and rotaxane 1

UV light (380 nm) irradiation on *E*-**1** (1.0×10^{-5} M in DMF) for 20 min generated *Z1*-**1**, which recovers to *E*-**1** on irradiation by 450 nm for 40 min. The change (Figure S8) is characterized by a rise in absorption at around 270 nm (ΔA_{270}=0.03) and a decrease in absorption at 350 nm (ΔA_{350}=0.062). The irradiation by 313 nm on *E*-**1** for 55 min generated another isomer *Z2*-**1**, which recovers to *E*-**1** on irradiation by 280 nm for 1.5 h. The change is also characterized by a rise in absorption at around 270 nm (ΔA_{270}=0.03) and a decrease in absorption at 350 nm (ΔA_{350}=0.052). Irradiation by 313 nm on *Z1*-**1** or irradiation by 380 nm on *Z2*-**1**, can generate *Z3*-**1**.

The change is characterized by a rise in absorption at around 270 nm (ΔA_{270}=0.058) and a decrease in absorption at 350 nm (ΔA_{350}=0.10).

Similarly, the irradiation at 380 nm (Figure S9) on the dumbbell **2** for 5 min caused an increase at around 270 nm (ΔA_{270}=0.05) and a decrease in absorption at 350 nm (ΔA_{350}=0.09), generating *Z1*-**2** rapidly, and the irradiation at 313 nm on the dumbbell **2** for 15 min caused an increase at around 270 nm (ΔA_{270}=0.045) and a decrease in absorption at 350 nm (ΔA_{350}=0.08), generating another isomer of the dumbbell *Z2*-**2**. In *Z3*-**2**, the absorption at 270 nm increases about 0.095 and the absorption at 350 nm decreases about 0.13 relatively to *E*-**2**. The fact that the spectral changes for the dumbbell **2** are more obvious than that for the rotaxane **1** indicates that the dumbbell **2** undergoes photoisomerization more easily by the UV irradiations. This is not surprising that the photoisomerization become more difficult in the presence of the α-CD ring.

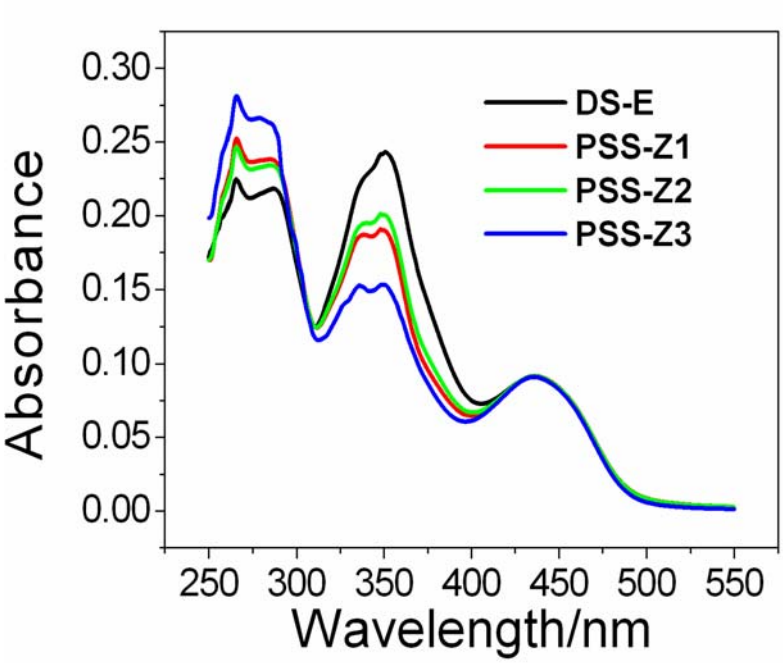

Figure S8. The absorption spectra of [2]rotaxane **1** in DMF (1×10^{-5} M) at 25 ºC. The black line is the spectrum without irradiation (*E*-**1**), the red line is the spectrum after irradiation at 380 nm for 20 min (*Z1*-**1**), the green line is the spectrum by irradiation at 313 nm for 55 min (*Z2*-**1**), and the blue line is after 380 nm for 20 min, then irradiation at 313 nm for 55 min (*Z3*-**1**), respectively.

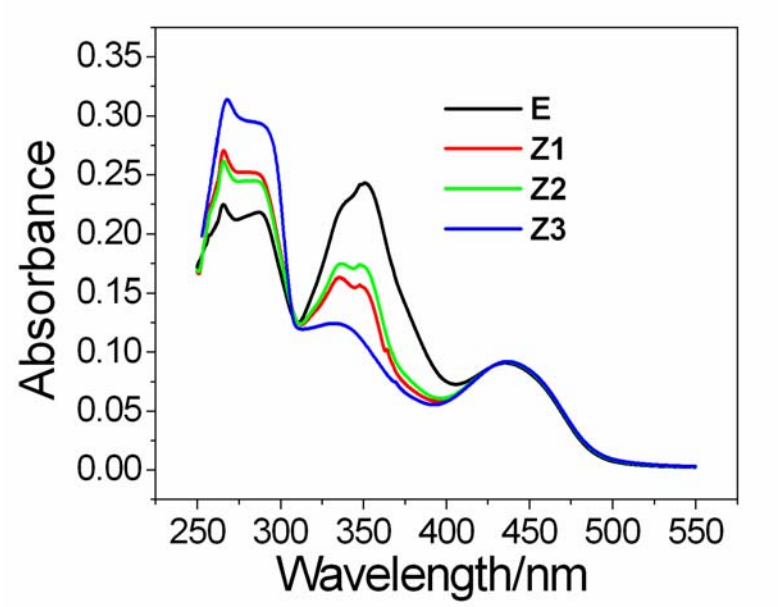

Figure S9. The absorption spectra of dumbbell **2** in DMF (1×10^{-5} M) at 25 ºC. The black line is the spectrum without irradiation (*E*-**2**), the red line is the spectrum after irradiation at 380 nm for 15 min (*Z1*-**2**), the green line is the spectrum by irradiation at 313 nm for 30 min (*Z2*-**2**), and the blue line is after 380 nm for 15 min, then irradiation at 313 nm for 30 min (*Z3*-**2**), respectively.

Fluorescence spectra

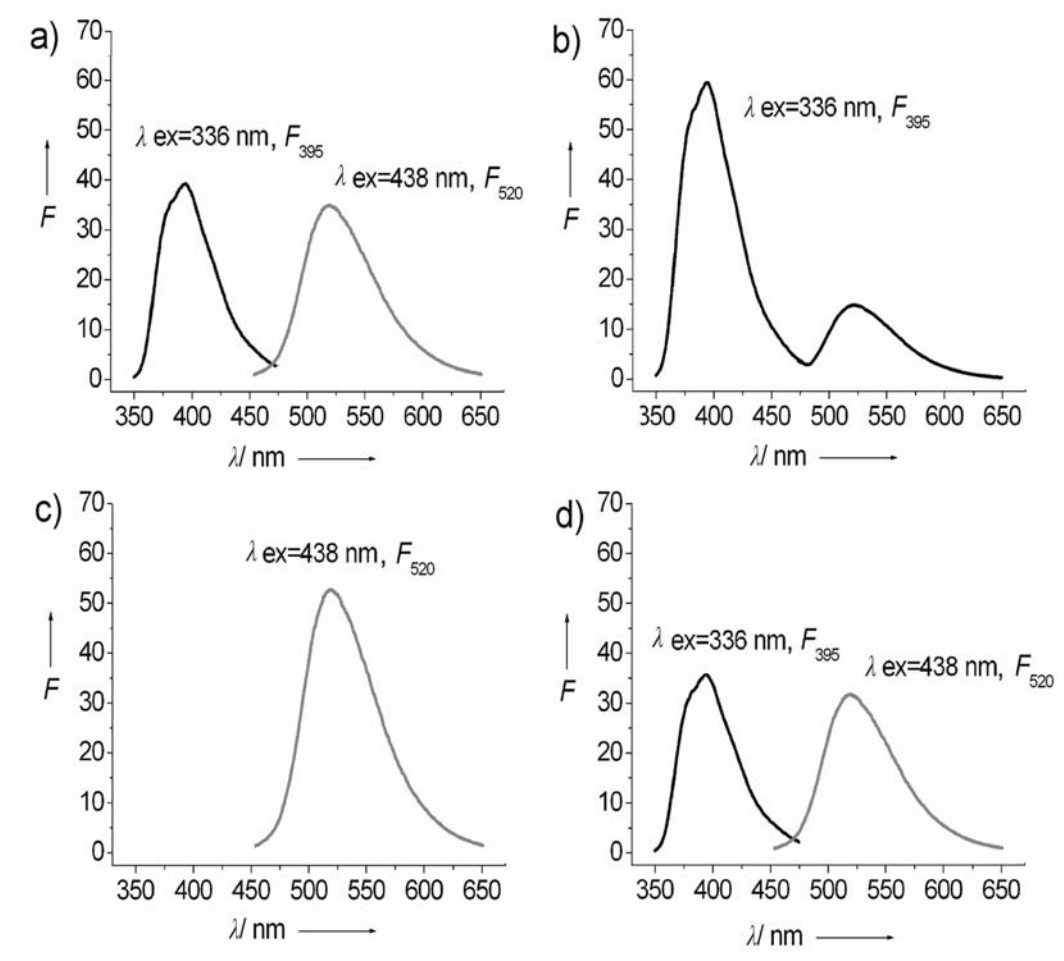

Figure S10. The fluorescence spectra of the "**N**" stopper (λ_{ex} = 438 nm, emission at λ_{max} = 520 nm) and the "**S**" stopper (λ_{ex} = 336 nm, emission at λ_{max} = 395 nm) of [2]rotaxane **1** solution (1.0×10^{-5} M in DMF). (a) DS-*E*-**1**; (b) PSS-*Z1*-**1**, irradiation *E*-**1** by 380 nm for 20 min; (c) PSS-*Z2*-**1**, irradiation *E*-**1** by 313 nm for 50 min; (d) PSS-*Z3*-**1**, irradiation *E*-**1** by 380 nm for 20 min, then irradiation by 313 nm for 50 min.

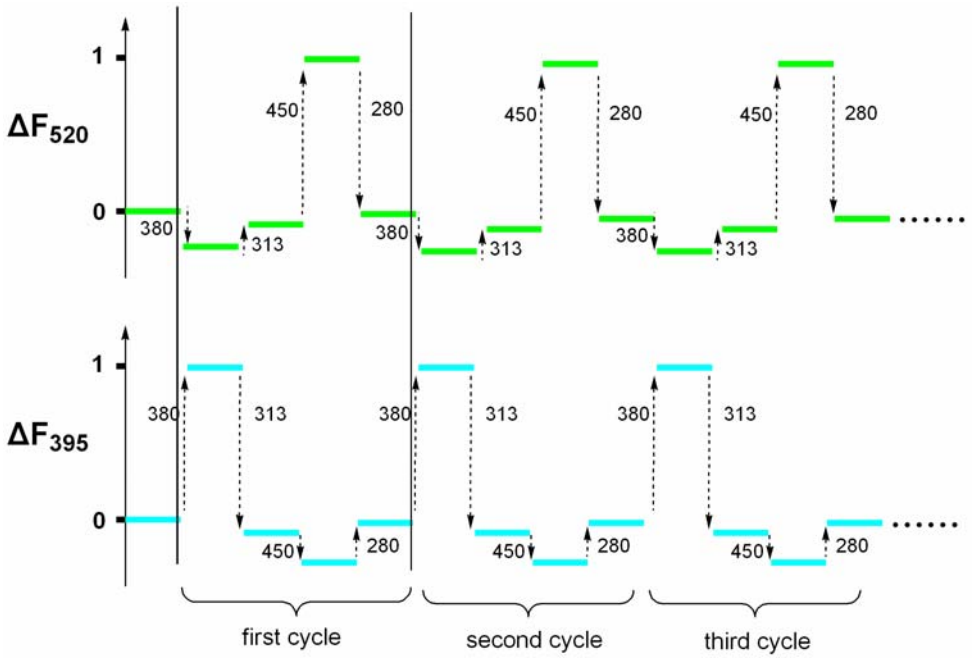

Figure S11. Changes in the fluorescence spectra of the "**N**" stopper (top, λ_{ex}=438 nm, emission at λ_{max}=520 nm) and the "**S**" stopper (below, λ_{ex}=336 nm, emission at λ_{max}=395 nm) of [2]rotaxane **1** solution (1.0×10^{-5} M in DMF) along with changes in irradiation cycle and light sources. In one cycle, UV light sources 380 nm, 313 nm, 450 nm and 280 nm are used sequentially. The photochemical processes are highly reproducible over more than 10 cycles.

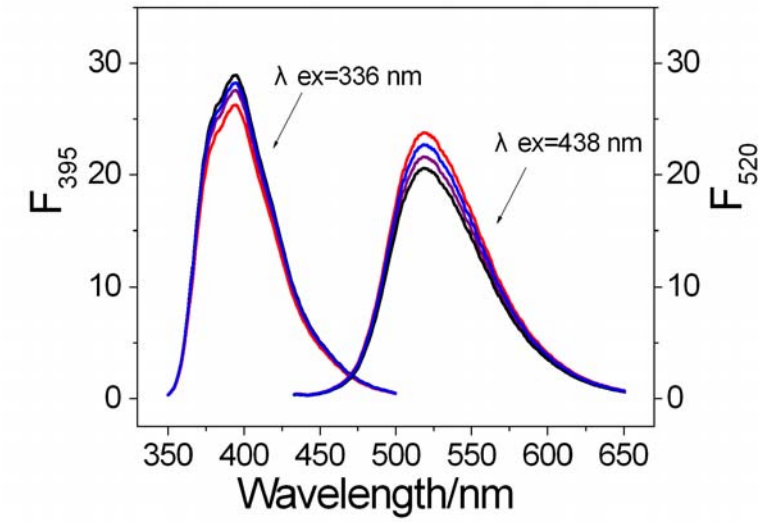

Figure S12. The fluorescence spectra of dumbbell **2** solution (1.0×10^{-5} M in DMF) in different states. The purple line stands for *E*-**2**, red for *Z1*-**2**, black for *Z2*-**2**, and blue for *Z3*-**2**. There is little change among these lines.

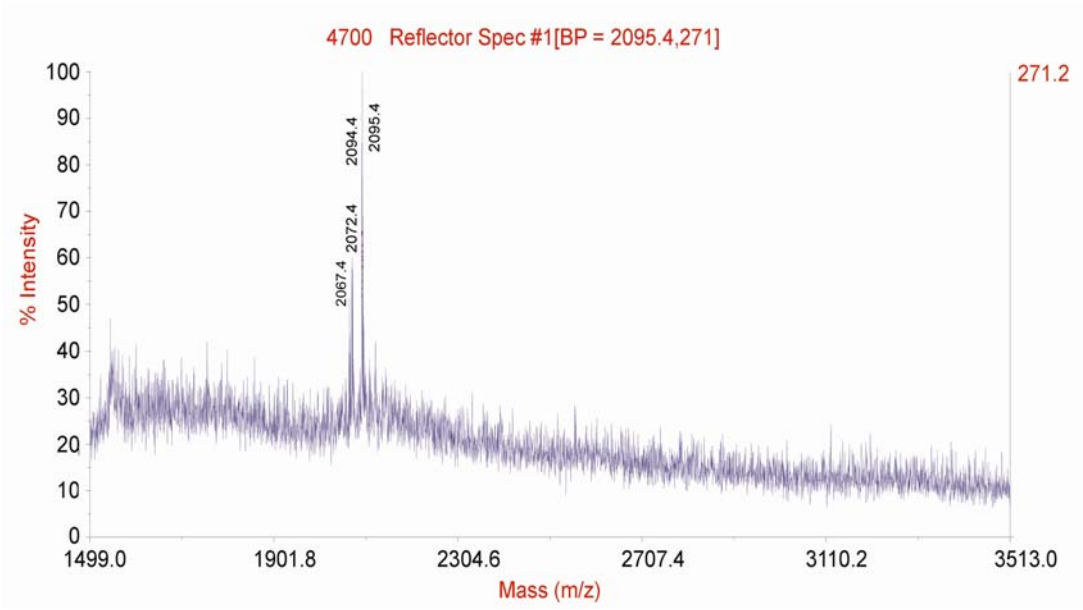

Figure S13. MALDI-TOF mass spectrum of [2]rotaxane **1**.

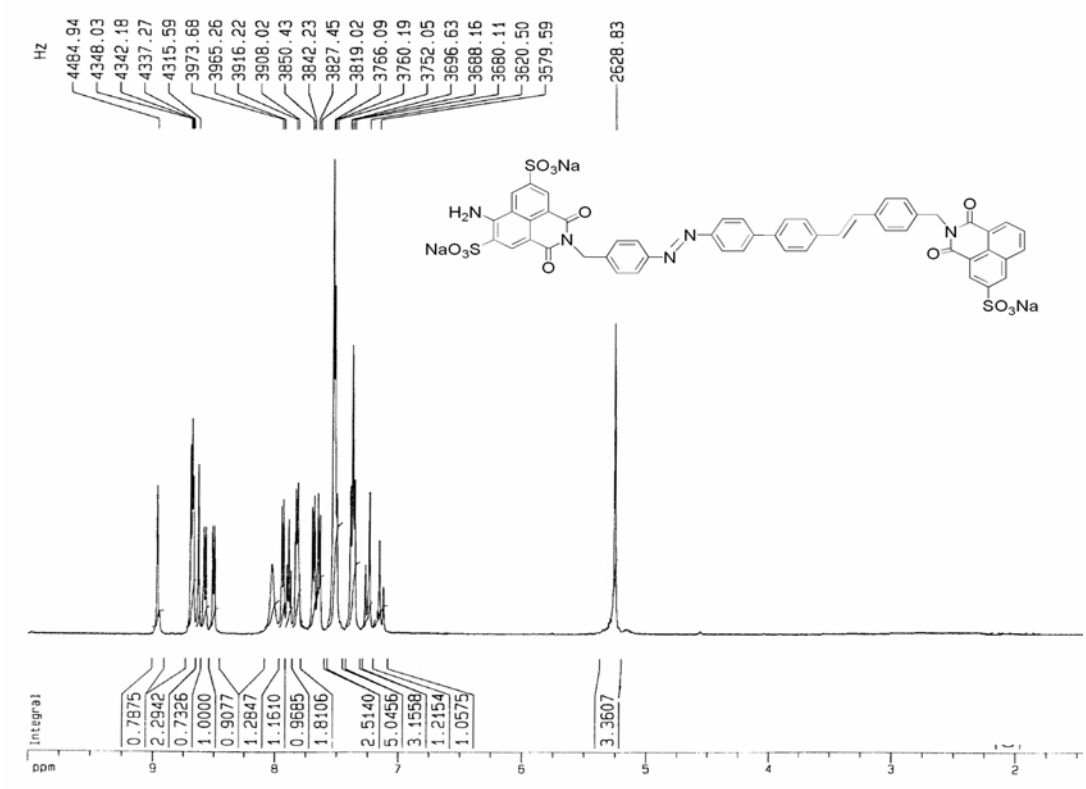

Figure S14. The ^{1}H NMR spectrum of dumbbell **2** (500 MHz in [D_6]-DMSO at 298 K).

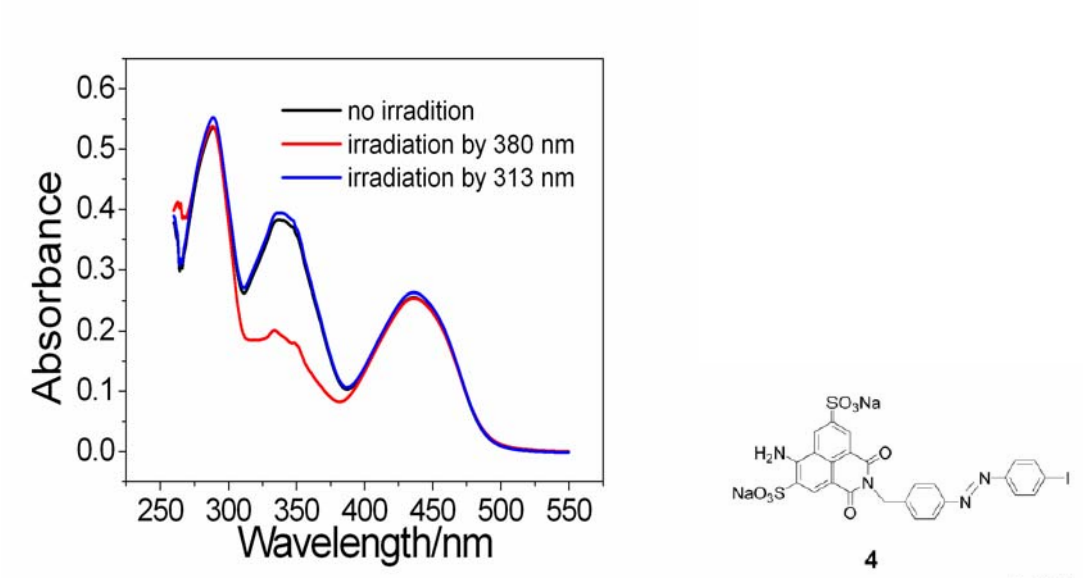

Figure S15. The absorption spectra of compound **4** in DMF (5×10^{-5} M) at 25 ºC. The black line is the spectrum without irradiation, the blue line is the spectrum after irradiation at 313 nm for 2 h, and the red line is the spectrum after irradiation at 380 nm for 30 min.

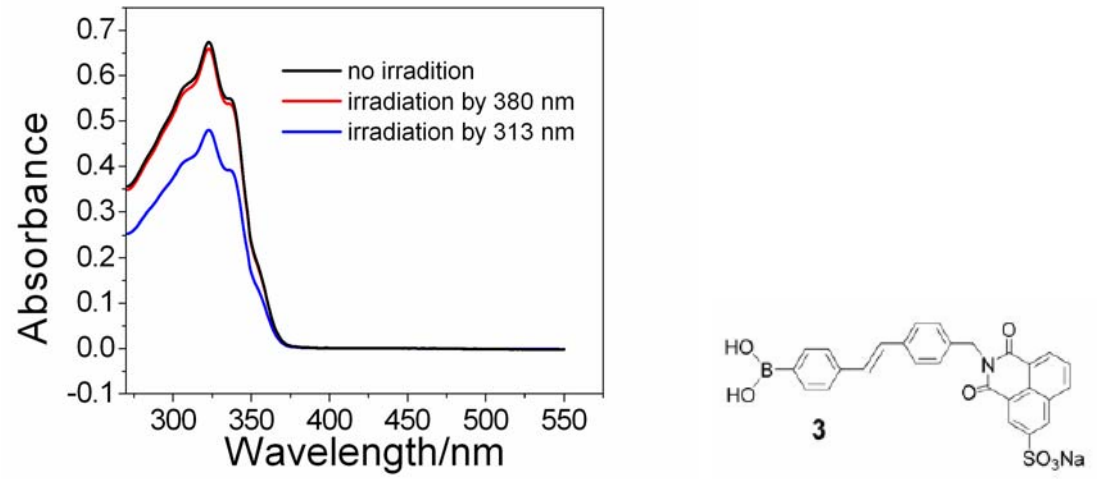

Figure S16. The absorption spectra of compound **3** in DMF (5×10^{-5} M) at 25 ºC. The black line is the spectrum without irradiation, the red line is the spectrum after irradiation at 380 nm for 2 h, and the blue line is the spectrum after irradiation at 313 nm for 30 min.

We have also studied the influence of α-CD on model "half-dumbbells" incorporating a single stopper and the azobenzene or the stilbene site in order to make clear how the macrocyclic component is actually affecting the fluorescence intensity.

As shown in Figure S17, adding excess α-CD to aqueous solution of compound **3** or **4** can enhance the fluorescence of the "**S**" or the "**N**" stopper about 1.7 times relative to the origin fluorescence. Although α-CD could provide steric protection to fluorophores limiting the efficiency of collisional quenching, little changes (Figure S18) in the fluorescence of the "**S**" or the "**N**" stopper were found when adding excess α-CD (10 equivalent) to aqueous solution of 1,8-naphthalimide- 5-sulfonic sodium salt (the "**S**" stopper) or 4-amino-1, 8-naphthalimide-3, 6-disulfonic disodium salt (the "**N**" stopper), which is probably because the two stoppers are too bulky to be included. So we confirm that the reason for the fluorescence changes is due to the rigidity of the α-CD ring, which limits the conformational motion around the methylene linkers and enhances the fluorescence intensity as a result.

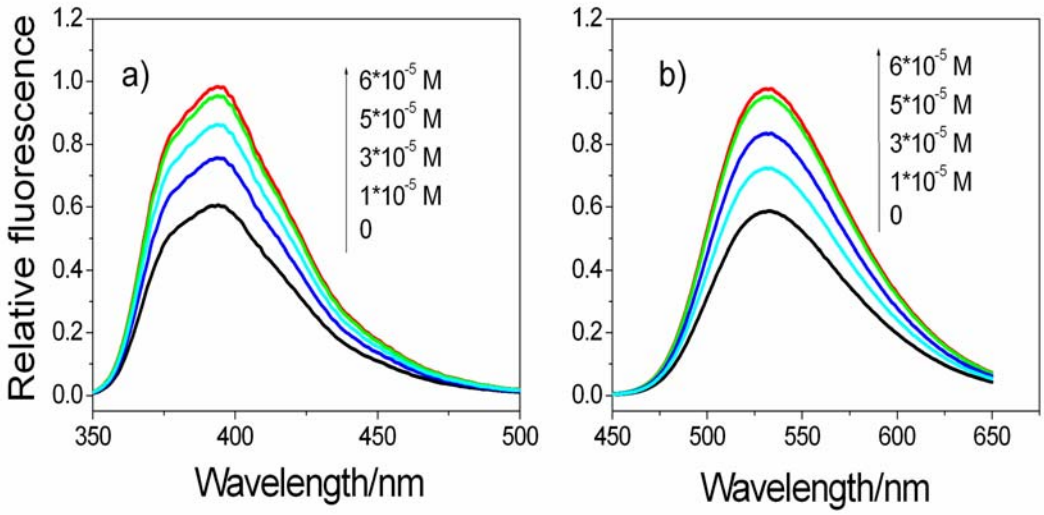

Figure S17. The relative fluorescence spectra of a) compound **2** (a half-dumbbell) in aqueous solution (1×10^{-5} M) at 25 ºC; b) compound **1** (other half-dumbbell) in aqueous solution (1×10^{-5} M) under the addition of α-CD or not. The fluorescence of each stopper enhances along with the increase of the α-CD concentration. The fluorescence of each stopper increases about 70% when reaching the balance state.

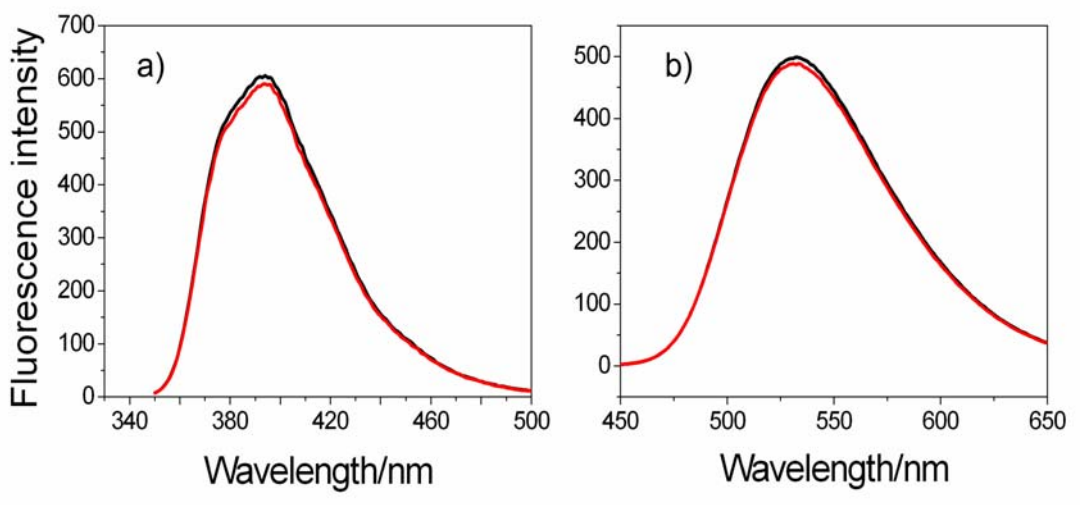

Figure S18. The fluorescence spectra of a) 1,8-naphthalimide- 5-sulfonic sodium salt—the "**S**" stopper in aqueous solution (9.1×10^{-6} M) at 25 ºC; b) 4-amino-1, 8-naphthalimide-3, 6-disulfonic disodium salt—the "**N**" stopper in aqueous solution (9.1×10^{-6} M) under the addition of 10 equivalent of α-CD or not. The red line is the spectrum without α-CD, the black line is the spectrum under the addition of 10 equivalent of α-CD. There is little fluorescence change before and after the addition of 10 equivalent of α-CD.

References

[S1] D.-H. Qu, Q.-C. Wang, X. Ma, H. Tian, *Chem. Eur. J.* **2005**, accepted (chem.200401313).

[S2] Q.-C. Wang, D.-H. Qu, J. Ren, K.-C. Chen, H. Tian, *Angew. Chem.* **2004**, *116*, 2715-2719; *Angew. Chem. Int. Ed.* **2004**, *43*, 2661-2665.

[S3] D.-H. Qu, Q.-C. Wang, J. Ren, H. Tian, *Org. Lett.* **2004**, *6*, 2085-2088.